---

**Proceedings Paper:**
Afzal, A, Zaidi, SAR, McLernon, DC et al. (2 more authors) (2017) M2M meets D2D: Harnessing D2D Interfaces for the Aggregation of M2M Data. In: 2017 IEEE International Conference on Communications. IEEE ICC'17: Bridging People, Communities, and Cultures, 21-25 May 2017, Paris, France. IEEE . ISBN 978-1-4673-8999-0

https://doi.org/10.1109/ICC.2017.7997135

---

# M2M meets D2D: Harnessing D2D Interfaces for the Aggregation of M2M Data

Asma Afzal[†◇], Syed Ali Raza Zaidi[†], Des McLernon[†], Mounir Ghogho[†‡] and Afef Feki[*]
[†] University of Leeds, United Kingdom [◇]CentraleSupélec, Gif-sur-Yvette, France [‡]International University of Rabat, Morocco,
[*]Mathematical and Algorithmic Sciences Lab, France Research Center, Huawei Technologies France SASU
Email: {elaaf, s.a.zaidi, d.c.mclernon, m.ghogho}@leeds.ac.uk, afef.feki@huawei.com

***Abstract*—Direct device-to-device (D2D) communication presents as an effective technique to reduce the load at the base station (BS) while ensuring reliable localized communication. In this paper, we propose a large-scale M2M data Aggregation and Trunking (MAT) scheme, whereby the user equipments (UEs) aggregate M2M data from the nearby MTDs and trunk this data along with their own data to the BS in the cellular uplink. We develop a comprehensive stochastic geometry framework by considering a Poisson hard sphere model for UE coverage. The main motivation of this model is to capture the fact that a UE can gather data from short range, low-power MTDs located only in its close proximity while ensuring that an MTD is associated to at most one UE. We explore the inherent trade-off between the time reserved for aggregation and successful trunking of data to the BS and compare our results with the baseline case where no aggregation mechanism is used. We show that while the baseline case of connecting a bulk of MTDs directly with the BS is prohibitive, MAT scheme can efficiently gather data from selected MTDs in a distributed manner.**

## I. Introduction

Machine-to-Machine (M2M) communication is the key enabler of the Internet of Things (IoTs) as sensing and actuating devices are present virtually in every industry nowadays. To fully realize the potential of IoTs, there is a need to develop sophisticated techniques to inter-connect these short range machine-type-devices (MTDs) with each other and the cloud to analyze their data and extract meaningful information. Cellular networks present as a suitable candidate to unify the data generated from MTDs due to their extensive global coverage. However, the existing cellular infrastructure is optimized for the Quality-of-Service (QoS) requirements of human-to-human (H2H) communication, which is based on fewer and longer sessions with the main focus on providing higher data rates. Conversely, MTDs are low power devices sending small amounts of data sporadically. Connecting a sheer bulk of MTDs with the cellular network will cause congestion at the core network. This poses a number of challenges on cellular networks and necessitates efficient resource management and clustering techniques with minimal signaling overhead [1].

A number of recent studies have proposed random access for MTDs over random access channel (RACH) in the cellular long-term evolution (LTE) [2], [3]. These techniques however, are not scalable for ultra dense scenarios due to increased collisions on RACH. Techniques like aggregation and clustering of MTDs have also proved to significantly mitigate the congestion problems [4]. Only recently, Device-to-Device (D2D) communication was identified as a fitting solution to aggregate M2M data and reduce the burden on the base stations (BSs) of scheduling and signaling [5]. D2D communication proximity service (ProSe) is an integral part of 4G and 5G networks as it enables low power devices in close proximity to communicate with each other [6]. Thus, cellular UEs can serve as ideal candidates for D2D enabled aggregators due to their abundance and high computation capabilities. A single cell, single UE framework for the aggregation and trunking of M2M traffic via D2D links with the UEs is provided in [7]. However, the analysis is only limited to a single cell and is not scalable as it does not take into account the physical locations of the MTDs and the UEs and more importantly, it does not consider the impact of interference from MTDs and UEs transmitting in other cells in aggregation and trunking phases respectively. Motivated by the above literature, we develop a large scale analytical framework for the aggregation of M2M data with the help of user equipments (UEs). The UEs collect M2M data by establishing D2D links with the nearby MTDs and pass this information to the base station (BS) with their own data.

The contributions of this paper are highlighted as follows. We propose a M2M data Aggregation and Trunking (MAT) scheme, where the UEs collect data from the MTDs and forward it along with their own data in cellular uplink (UL) radio resources. The Voronoi tessellation assumption commonly used for BS coverage regions in cellular networks [8] is not suitable for UE coverage modeling due to lower sensitivity of UE receivers and low MTD transmit power. A number of works on wireless networks assume some kind of interaction between the devices to model them as clustered point process. Popular choices for clustered processes include Matern cluster process [9] and Thomas process [10]. The deployment of dense, large-scale MTD networks, however, is not necessarily dependent on the presence of UEs. Therefore, we develop a clustering technique using Poisson hard sphere (PHS) model to represent the coverage regions of the UEs after the MTDs have been homogeneously deployed in a given area. For the aggregation phase, we consider that the MTD transmissions

This work has been supported by the UK Engineering and Physical Sciences Research Council (EPSRC) grant EP/P511341/1 for the University of Leeds Institutional Support under EPSRC Prosperities Outcome Framework. All data are provided in full in the results section of this paper.

are coordinated by the UEs. The coordinated MTD transmissions do not interfere with each other, but cause extensive signaling and control overhead at the BS. For the trunking phase, we assume that the UEs employ constrained UL channel inversion power control. We obtain tight approximations of the rate coverage for both the aggregation and trunking phases. We explore the inherent trade-off between the time reserved for aggregation by the UEs and the successful data delivery in both the aggregation (MTD-UE) and trunking phases (UE-BS). In fact, larger aggregation periods results in better aggregation opportunities from multiple MTDs but at the cost of trunking performance degradation.

## II. The MAT Scheme

We propose a novel M2M data Aggregation and Trunking (MAT) scheme, where the UEs relay the M2M data to the BS along with their own data. We consider that the BSs, UEs and the MTDs are distributed independently in $\mathbb{R}^2$ according to homogeneous Poisson point processes (HPPPs) $\Phi_b$, $\Phi_u$, and $\Phi_m$ with intensities $\lambda_b$, $\lambda_u$ and $\lambda_m$ respectively. In our proposed scheme we focus in the cellular UL. The UEs associate to the nearest BS, which implies that the macrocells form a Voronoi tessellation in $\mathbb{R}^2$. The transmissions from both the MTDs and UEs suffer form channel impairments including small scale Rayleigh fading and path loss. As a consequence, the channel power gain $h \sim \exp(1)$ is a unit mean exponential random variable. Throughout this paper, we assume a simple power law path loss function $r^{-\alpha}$ for a distance separation $r$ where $\alpha$ is the path loss exponent. We consider the same value of $\alpha$ to account for MTD-UE and UE-BS links, however, the presented framework can be easily extended to account for various propagation environments. The key stages involved in our proposed MAT scheme are presented as follows.

### A. Clustering MTDs using Poisson Hard Sphere (PHS) Model

The first step is to determine how a UE collects data from its nearby MTDs and how we can ensure that each MTD is associated to at most one UE. According to the PHS model in 2-d, the interiors of the disks centered at the points of the parent process do not overlap almost surely (a.s.). The nearest neighbor model (NNM) proposed by Stienen in [11] is a type of PHS extensively used in disk packing and percolation problems. In case of NNM, the diameter of the disk centered at a given particle is the distance to it's nearest neighbor of the same process. To understand this better in the context of wireless networks, consider a UE $z_j$, where $z_j \in \Phi_u$. The radius of the Stienen disk of $z_j$ is then given as

$$X = \min_{z_l} \eta \|z_j - z_l\|,\ z_l, z_j \in \Phi_u, l \neq j, \tag{1}$$

where the Stienen cell (S-cell) $\mathcal{B}_{z_j} = \left\{y \in b(z_j, X),\ y \in \mathbb{R}^2\right\}$ is a disk of radius $X$ and $\eta = 1/2$ for the NNM. We extend this model to a more general case where the scalar $\eta$ may take any value from the range $0 < \eta \leq 1/2$. This gives us control on accurately modeling the coverage regions of UEs especially when the UEs are sparsely populated. Notice that for any value of $\eta$, the UE S-cells form disjoint sets such that $\mathcal{B}_{z_l} \cap \mathcal{B}_{z_j} = \emptyset, \forall z_j \neq z_l$. This implies that the MTDs inside a UE's S-cell are only associated to it.

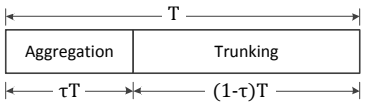


Figure 1. Division of the uplink time slot

The distribution $f_X(x)$ of the radius of the S-cell can be quantified using the concept of void probability of Poisson processes. The probability that the radius $X$ exceeds a certain threshold $x$ is the probability that there is no UE at a distance $\eta^{-1}x$ from the given UE. It can be expressed as $\mathbb{P}[X \geq x] = \exp\left(-\lambda_u \pi \eta^{-2} x^2\right)$. The resulting process of MTDs inside the S-cells constitute a modified Matern cluster process [9], where the radius of the disks is random and is distributed according to $f_X(x)$. Using the S-cell radius distribution of the radius of the S-cell, the probability mass function of the number of MTDs inside an arbitrary S-cell can be easilty derived using the fact that the MTDs are Poisson distributed in a S-cell with mean measure $\lambda_m \pi x^2$. It is given as [12] $\mathbb{P}[N_m = n] = \mu(1+\mu)^{-n-1}$, where $\mu = \lambda_u \eta^{-2}/\lambda_m$.

### B. Communication Framework

We consider that the UL time slot is further divided into two slots as shown in Fig. 1. In the first slot, the UEs establish D2D links with the nearby MTDs to aggregate the M2M data. In the second slot, regular UL transmission takes place whereby UEs employ power control to transmit their own data as well as the collected M2M data to the BS. We now describe the transmission schemes for aggregation and trunking phases.

*1) Aggregation:* We consider that the MTDs transmit at a fixed power $P_m$ and MTD transmissions are multiplexed (MX) in frequency or time. The MTDs employ frequency division multiple access (FDMA) or time division multiple access (TDMA). Both TDMA and FDMA result in the same average data rate so we do not make further distinction between the two in the rest of the paper. To account for the extra signaling for multiplexed transmission, we consider that the available aggregation time $T_{eff} = \tau T - kT_{sig}$ is effectively smaller by $kT_{sig}$, where $T_{sig}$ is the time spent by the MTDs in contending for a transmit opportunity and channel reservation by the UE.

*2) Trunking:* In this phase, the UEs transmit their own data along with the collected M2M to the BS. We consider that the cellular bandwidth $W_u$ is equally divided among the UEs inside a macrocell and there in no intra-cell interference. For energy efficient operation, the UEs employ UL channel channel inversion power control. The transmit power under the truncated UL channel inversion power control is written as

$$P_u = \min\left(P_u^{max}, \rho_0 l(y)^{-1}\right). \tag{2}$$

Notice that that the transmit power is constrained by the upper limit $P_u^{max}$, which is the maximum transmit power of a UE and $l(y) = y^{-\alpha}$ is the path loss when the UE and the BS are separated by a distance $y$. The distribution

of the distance between an arbitrary UE and its associated BS follows a well known Rayleigh distribution and is given as [8] $f_Y(y) = 2\pi\lambda_b y \exp\left(-\lambda_b \pi y^2\right)$. The term $\rho_0$ is the normalizing factor depending on the receiver sensitivity of the BS. We can see from (2) that the UEs only at a certain distance $R_{max} = \left[\frac{P_u^{max}}{\rho_0}\right]^{1/\alpha}$ can successfully invert the path loss. The UEs outside a disk of radius $R_{max}$ will transmit at maximum power. Unlike the truncated channel inversion power control presented in [13], where the UEs farther from $R_{max}$ are forced to go into outage, we present a more realistic power control scheme as the disadvantaged UEs still get a chance to transmit.

### C. Probability of Successful Aggregation and Trunking (PSAT)

For cellular downlink scenarios, network operators are interested in load balancing and maximizing the rate experienced by a UE and the overall area spectral efficiency of the network [14]. On the contrary, the performance metrics are quite different for cellular UL and M2M applications, where ensuring reliability and enhancing connectivity is the primary focus. Based on this criteria, we define a key performance determining metric for the analysis of the aggregation and trunking communication framework described above.

**Definition 1.** PSAT: The probability that a UE is able to successfully aggregate M2M data from $k$ MTDs in time $\tau T$ and can trunk it along with its own data in time $(1-\tau)T$, can be expressed as the product of rate coverage in aggregation and trunking phases. It is given as $\mathcal{P}_k^{MX} = \mathcal{R}_a^{MX} \times \mathcal{R}_t$, where, $\mathcal{R}_a^{MX}$ is the rate coverage in aggregation phase and $\mathcal{R}_t$ is the rate coverage in trunking phase. The description and derivation of the rate coverage for each phase is given in the following subsections.

*1) Aggregation Phase:* In this phase, the MTDs within the UEs S-cell transmit to it. Assuming that the MTDs transmit a fixed payload of size $D_m$ bits using the available bandwidth $W_m$ in time $\tau T$, aggregation is successful only when the the M2M data from $k$ MTDs is successfully decoded. We consider Shannon's capacity formulation to characterize the rate coverage for various transmission schemes. The rate coverage for multiplexed transmission can be represented as

$$\begin{aligned}\mathcal{R}_a^{MX} &= \left(\mathbb{P}\left[\frac{W_m}{k}\log_2(1+SIR_a^{MX}) \geq \frac{D_m}{T_{eff}}\right]\right)^k \\ &= \left(\mathbb{P}\left[SIR_a^{MX} \geq \theta_a^{MX}\right]\right)^k, \end{aligned} \quad (3)$$

where $\theta_a^{MX} = 2^{\frac{kDm}{W_m T_{eff}}} - 1$ and $T_{eff} = \tau T - kT_{sig}$ is the effective time available for MTD transmission after the signaling and channel reservation for $k$ MTDs. The SIR of the received signal at the UE is given as $SIR_a^{MX} = h\, R_{arb}^{-\alpha}/I_m$, where $I_m = \sum_{w_j \in \Phi_m^{int}} h_j ||\omega_j||^{-\alpha}$ is the aggregate interference power experienced by the UE from MTDs in the other S-cells and $R_{arb}$ is the distance between an arbitrary MTD and its closest UE, given that the MTD is located inside the UE's S-cell. The distribution of this distance is given by the following Lemma.

**Lemma 1.** *If an arbitrarily selected MTD is present inside the coverage region of a UE, the distribution of the distance between the UE and the MTD is given as*

$$f_{R_{arb}}(r) = 2\pi r \lambda_{arb} \exp\left(-\pi r^2 \lambda_{arb}\right), \quad (4)$$

*where* $\lambda_{arb} = \lambda_u \left(1+\eta^{-2}\right)$.

*Proof:* The unconstrained distribution of the distance between an arbitrary MTD and the nearest UE is Rayleigh distributed and is given as $f_{R_{uncon}}(r) = 2\pi r\, \lambda_u \exp\left(-\lambda_u \pi r^2\right)$. However, in this case, the MTD must also lie in the S-cell of the nearest UE. We need to find $\mathbb{P}\left[R_{uncon} = r | X \geq R_{uncon}\right]$, which is the PDF of distance with the condition that the S-cell encapsulates the arbitrary MTD. Therefore, we have

$$f_{R_{arb}}(r) = \frac{\mathbb{P}\left[X \geq r\right]\mathbb{P}\left[R_{uncon} = r\right]}{\mathbb{P}\left[X \geq R_{uncon}\right]}, \quad (5)$$

where $\mathbb{P}\left[X \geq r\right] = \exp\left(\lambda_u \pi r^2 \eta^{-2}\right)$ and $\mathbb{P}\left[X \geq R_{uncon}\right] = \int_0^\infty \left(1 - F_X(t)\right) f_{R_{uncon}}(t)\, dt = \left(1+\eta^{-2}\right)^{-1}$. Substituting these expressions in (5) gives (4). ∎

Lemma 1 reveals that the distribution with S-cell restrictions differ with the unconstrained case HPPP case in density only. As $\lambda_{arb} \geq \lambda_u$, the average distance between UE and an arbitrary MTD is smaller. This implies that the current network with S-cell boundary restrictions can be translated into a denser unconstrained HPPP network. The following proposition gives the coverage probability for the aggregation phase with MX transmission.

**Proposition 1.** *For a given SIR threshold $\theta$, the probability that the UE successfully decodes the data from an arbitrary MTD within its S-cell is given as*

$$\mathcal{S}_a^{MX}(\theta) \approx \int_0^\infty \exp\left(-2\pi\lambda_m^{int}\mathbb{E}_Q\left[\mathcal{C}\left(\alpha, s_a, q\right)\right]\right) f_{R_{arb}}(r) dr, \quad (6)$$

*where $Q$ is distributed according to $f_Q(q) = 2\pi\lambda_m^{int} q \exp\left(-\lambda_m^{int}\pi q^2\right)$, $\lambda_m^{int} = \lambda_u(1+\mu)^{-1}$ and $\mathcal{C}(\alpha,\beta,d) = \frac{\beta d^{(2-\alpha)}}{(\alpha-2)}\mathcal{F}\left(\alpha, \frac{d^\alpha}{\beta}\right)$ where $\mathcal{F}\left(\alpha, \frac{d^\alpha}{\beta}\right) = {}_2F_1\left(1, 1-\frac{2}{\alpha}; 2-\frac{2}{\alpha}; -\beta d^{-\alpha}\right)$ and ${}_2F_1\left(.,.;.;.\right)$ is the generalized hypergeometric function.*

*Proof:* Please refer to Appendix A. ∎

*2) Trunking Phase:* In this phase, the UEs transmit the data collected from $k$ MTDs along with their own data to the BS. Assuming the UEs require a fixed data rate $R_u = D_u/T$, the rate coverage in trunking phase can be written as $\mathbb{E}_{N_u}\left[\mathbb{P}\left[SIR_t \geq \theta_t\right]\right]$, where $\theta_t = 2^{\frac{n(D_u+kD_m)}{W_u(1-\tau)T}} - 1$ and $N_u$ is the number of UEs inside a macrocell to which the arbitrarily chosen UE belongs (Ref (3) in [15]). To simplify things, we adopt the mean-load approximation as in [14]. The average number of UEs inside a macrocell is given by $N_u^{avg} = 1 + 1.28\,\lambda_u/\lambda_b$. Therefore, the rate coverage simplifies to

$$\mathcal{R}_t = \mathbb{P}\left[\frac{W_u}{N_u^{avg}}\log_2(1+SIR_t) \geq \frac{D_u + kD_m}{(1-\tau)T}\right], \quad (7)$$

| Parameter | Value |
|---|---|
| Densities of BS $\lambda_m$, UE $\lambda_u$, and MTD, $\lambda_m$, Ratio of densities $\lambda_m/\lambda_u$ | $[2, 20, 200]/\pi 500^2$, 1 |
| Max. transmit power of MTD $P_m$, UE $P_u^{max}$ and BS receiver sensitivity $\rho_0$ | $[-18, 23, -80]$ dBm |
| PHS coefficient $\eta$, Path loss exponent $\alpha$, UL slot fraction $\tau$ | 1/2, 4, 0.2 |
| MTD and UE bandwidth $W_m, W_u$ | 180 kHz, 10 MHz |
| M2M Payload $D_m$, Desired UE data rate for its own data $R_u$ | 100 bits, 10 Kbps |
| UL slot time period $T$, Signaling time per MTD $T_{sig}$ | 1 ms, 0.1 ms |

Table I
LIST OF SIMULATION PARAMETERS

and $\theta_t = 2^{\frac{N_u^{avg}(D_u+kD_m)}{W_u(1-\tau)T}} - 1$. We will make use of this approximation throughout the course of this paper. The SIR at the BS in trunking phase can be represented as $SIR_t = \frac{P_u h Y^{-\alpha}}{I_u}$,where $P_u$ is the variable transmit power given in (2) depending on the distance $Y$ between the UE and the BS it is associated with and $I_u = \sum_{z_j \in \Phi_u^{int}} P_{u,j} h_j \, ||z_j||^{-\alpha}$, where $||z_j||$ is the distance of the interfering UE $z_j$ from the typical BS and $\Phi_u^{int}$ comprises of the interfering UEs from other cells as we assume that there is no intra-cell interference. In the following Lemma, we obtain the average power transmitted by a UE which will help characterize the coverage in trunking phase.

**Lemma 2.** *Under constrained UL channel inversion power control, the average power transmitted by a UE is given as*

$$P_u^{avg} = \frac{\rho_0 \Gamma(\delta)}{(\lambda_b \pi)^{\alpha/2}} \gamma\left(\lambda_b \pi R_{max}^2, \delta\right) + P_u^{max} \exp\left(-\lambda_b \pi R_{max}^2\right), \tag{8}$$

*where* $\delta = 1 + \alpha/2$, $R_{max} = \left[\frac{P_u^{max}}{\rho_0}\right]^{1/\alpha}$ *and* $\gamma(b,a) = 1/\Gamma(a) \int_0^b t^{a-1} \exp(-t)\, dt$ *is the normalized lower incomplete gamma function.*

*Proof:* The average transmit power is calculated by taking expectation of (2) with respect to $Y$. ∎

The coverage probability for a generic UL with constrained channel inversion power control is given by the following proposition.

**Proposition 2.** *When a generic user transmits to the nearest BS by employing constrained channel inversion power control, the probability that the BS can successfully decode this signal can be expressed as*

$$\mathcal{S}_t(\theta) = \int_0^{R_{max}} \exp\left(-2\pi\lambda_b \mathbb{E}_{P_u}\left[\mathcal{C}(\alpha, s_1 P_u, y)\right]\right) f_Y(y) dy + \int_{R_{max}}^{\infty} \exp\left(-2\pi\lambda_b \mathbb{E}_{P_u}\left[\mathcal{C}(\alpha, s_2 P_u, y)\right]\right) f_Y(y) dy \tag{9}$$

*where* $s_1 = \theta/\rho_0$, *for* $0 \le y \le R_{max}$ *and* $s_2 = \theta y^\alpha / P_u^{max}$ *for* $y > R_{max}$.

*Proof:* The sketch of the proof is as follows. The conditional coverage probability of the UE can be expressed as

$$\mathcal{S}_t(\theta)|y = \begin{cases} \mathbb{P}\left[\frac{\rho_0 h}{I_u} \ge \theta\right] = \mathcal{L}_{I_u}(s_1) & 0 \le y \le R_{max}, \\ \mathbb{P}\left[\frac{P_u^{max} h\, y^{-\alpha}}{I_u} \ge \theta\right] = \mathcal{L}_{I_u}(s_2) & y > R_{max}, \end{cases}$$

Here, $\mathcal{L}_{I_u}(.)$ is the Laplace transform of the interference experienced by the BS from the active UEs in other macrocells. We assume the interfering UEs comprise a HPPP [1] $\Phi_u^{int}$ with the intensity equal to the BS intensity $\left(\lambda_u^{int} = \lambda_b\right)$. After using similar mathematical manipulations as the proof of Prop. 2, we obtain (9). ∎

**Corollary 1.** *The UL coverage probability can be simplified as*

$$\mathcal{S}_t(\theta) \approx \int_0^{R_{max}} \exp\left(-2\pi\lambda_b \mathcal{C}(\alpha, s_1 P_u^{avg}, y)\right) f_Y(y) dy + \int_{R_{max}}^{\infty} \exp\left(-2\pi\lambda_b \mathcal{C}(\alpha, s_2 P_u^{avg}, y)\right) f_Y(y) dy \tag{10}$$

*Proof:* The function inside the integral in $\mathcal{C}(\alpha, s_1 P_u, y) = \int_y^\infty \frac{\nu}{1+(s_t P_u)^{-1} \nu^\alpha} d\nu$ is strictly concave in $P_u$. We employ Jensen's inequality in (9) to shift the expectation with respect to $P_u$ inside to obtain a lower bound for coverage. ∎

## III. RESULTS AND DISCUSSION

In this section, we verify our analysis using Monte-Carlo simulations and provide some useful design insights for the aggregation and trunking framework. To compute the distribution of distance and coverage, we conduct $10^4$ iterations. In each iteration, the BSs, UEs and MTDs are distributed independently according to HPPPs with densities $\lambda_{b,}$ $\lambda_u$ and $\lambda_m$ respectively in a circular area of radius 1.5 km. The list of simulation parameters and their description is given in table I unless stated otherwise. We begin with the verification of Lemma 1. For the distance between the UE and an arbitrarily distributed MTD, we generate the S-cells and fix the location of the MTD at the origin. The distance between the UE and MTD is recorded if the MTD lies inside the nearest UE's S-cell. The iterations where the MTD lies outside the S-cell are ignored. For clear comparison with the unconstrained HPPP case, we obtain the cumulative distribution function (CDF) of the distance $R_{arb}$, which is given as $F_{R_{arb}}(r) = 1 - \exp\left(-\lambda_{arb}\pi r^2\right)$, where $\Gamma(a,b) = \int_b^\infty t^{a-1} \exp(-t)\, dt$ is the upper incomplete gamma function. As shown in Fig. 2, the simulation accurately matches our analytical results for various values of $\eta$ and $i$. As $\eta$ decreases, the size of S-cell also decreases and therefore, the distance between the UE and MTDs inside the cell also decreases. As expected, the distance between the UE and an arbitrary MTD within its S-cell is statistically smaller compared to the unconstrained case.

[1] Even though the HPPP assumption does not encapsulate the correlations in the UE locations, it is shown to be quite accurate in [13]

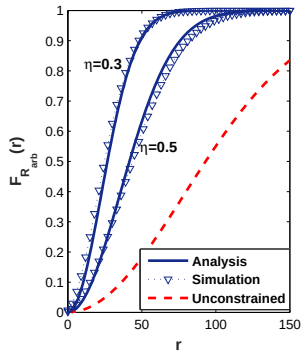


Figure 2. CDF of the distance between the UE and an arbitrarily distributed MTD inside the S-cell: $\lambda_m = 500/\pi 500^2$

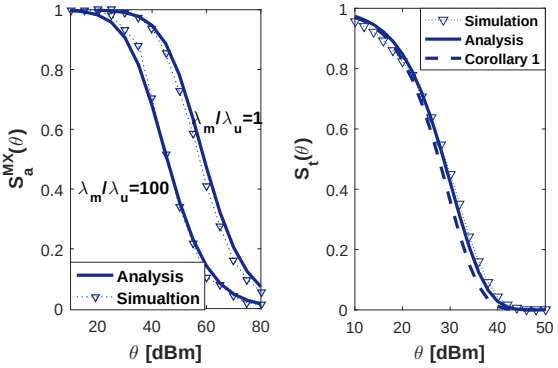


Figure 3. SIR coverage probability. Aggregation (left), trunking (right).

Moving on, we validate the expressions for SIR coverage probability for the aggregation and trunking phases derived in Propositions 1, and 2 in Fig. 3. The plots demonstrate a strong agreement between the simulations and the derived analytical results. Fig. 3 further shows that the coverage probability in aggregation phase $\mathcal{S}_a^{MX}$ decreases when $\lambda_m/\lambda_u$ increases. The drop in $\mathcal{S}_a^{MX}$ is attributed to the increase in the interferer intensity $\lambda_m^{int} = \lambda_u(1+\mu)^{-1}$ as $\lambda_m/\lambda_u \to \infty$, $\lambda_m^{int} = \lambda_u$. This implies that each S-cell has at least one MTD transmitting to its UE. On the contrary, the trunking coverage $\mathcal{S}_t$ does not depend on $\lambda_u$ or $\lambda_m$ as evident from (9) and (10). In case of trunking, Fig. 3 reveals that the equi-dense HPPP assumption in (10) for the interfering UEs is quite accurate. The simplified lower bound derived in Corollary 1 is also in good agreement with the analysis and simulations. Notice that the coverage for the aggregation phase is better compared to the trunking phase. This is because the smaller path loss between the UE-MTD link improves the received signal strength at the aggregation stage.

After validation of the preliminary results using network simulations, we investigate the factors affecting PSAT and the scenarios where aggregation and trunking is feasible. Fig. 4 explores the effect of $k$ and $\tau$ (the fraction of UL time slot reserved for aggregation) on the rate coverage. The results are intuitive as the increase in $k$ causes both $\mathcal{R}_t$ and $\mathcal{R}_a^{MX}$ to

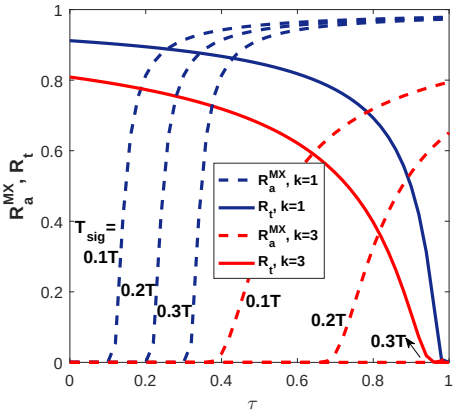


Figure 4. Rate Coverage in aggregation and trunking phases.

degrade. However, for a given $k$, an interesting trade off in $\tau$ is revealed. As we increase $\tau$, the trunking rate coverage $\mathcal{R}_t$ drops, while the aggregation rate coverage $\mathcal{R}_a^{MX}$ increases. This is because a higher $\tau$ corresponds to a better aggregation opportunity for $k$ MTDs as $\theta_a^{MX}$ decreases whereas, it results in a degraded trunking performance as $\theta_t$ increases because lesser time is available for trunking UE and M2M data from $k$ MTDs $(D_u + kD_m)$. Hence, there must exist an optimal $\tau = \tau_{MX}^*$ which maximizes $\mathcal{P}_k^{MX}$. Another important factor to take into consideration while deciding the transmission scheme in aggregation phase is the signaling overhead in MX case. Even though MX transmission is generally more robust, we see that even slightly increasing $T_{sig}$ results in complete outage for small values of $\tau$. This is because there is no time left for data transfer as $\tau T \leq kT_{sig}$.

In Fig. 5, we study the variation in $\mathcal{P}_k^{MX}$ with respect to $\tau$ and $k$. As expected, the maximum achievable PSAT decreases with the increase in $k$ as both $\mathcal{R}_t$ and $\mathcal{R}_a^{MX}$ decrease. The increase in $k$ also causes $\tau_{MX}^*$ to increase and the optimal point shifts further right. This implies that the degradation in $\mathcal{R}_a^{MX}$ is higher than in $\mathcal{R}_t$. We also compare $\mathcal{P}_a^{MX}$ with the baseline case, where the MTDs transmit to the BS directly with power $P_m$ without hierarchical aggregation. For fairness in comparison, we consider that the BS has to decode the data from $kN_u^{avg}$ MTDs, which is the average number of of active MTDs inside the cell under the MAT scheme. Because of the centralized control, only one MTD transmits to the BS at a given snapshot of the network. Therefore, the rate coverage probability for the baseline case is given by $\mathcal{P}_{Base} = \mathbb{E}_Y\left[\exp\left(-2\pi\lambda_b \mathcal{C}\left(\alpha, \theta_{a,B}^{MX} y^\alpha, y\right)\right]^{kN_u^{avg}}$ [8], where $\theta_{a,B}^{MX} = 2^{\frac{k N_u^{avg} D_m}{W_m T}} - 1$. We observe that when $k = 1$, and the average number of MTDs inside the cell is small, no hierarchical aggregation is required. However, as $k$ increases, our proposed MAT scheme provides exceedingly good performance compared to the baseline. This is because, coordinating access for a high number of MTDs at the BS will cause congestion at the BS and result in performance

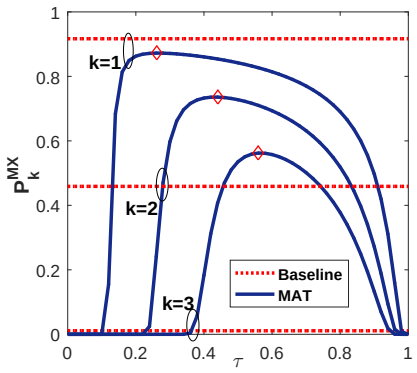


Figure 5. Effect of MTD and UE densities on $\mathcal{P}_k^{MX}$.

degradation. For $k = 3$, the probability of successful data delivery is about 55% better than what can be achieved with the baseline case.

## IV. Conclusion

In this paper, we propose the MAT scheme for aggregation and trunking of M2M data with the help of D2D links in the cellular uplink. A PHS model is formulated to characterize the coverage regions of UEs performing D2D communications with its MTDs. The performance evaluation also accounts for the scheduling and signaling overhead for coordinating MTD transmission at the UEs. For the proposed MAT scheme, the fraction of time slot reserved for data aggregation by the UEs plays a crucial role in determining the probability of successful data delivery at the BS. Simulation results show the efficiency of the proposed MAT scheme with huge performance gains compared to the baseline case, where the MTD transmit directly to the BS.

## Appendix A
## Proof of Proposition 1

The coverage probability for MX transmission of MTDs can be characterized as $\mathcal{S}_a^{MX}(\theta) = \mathbb{E}_{R_{arb}}\left[\frac{h\, r^{-\alpha}}{I_m} \geq \theta\right]$. Since the channel power $h$ is exponentially distributed, $\mathcal{S}_a^{MX}(\theta) = \mathbb{E}_{R_{arb}}\left[\mathcal{L}_{I_m}(s_a)\right]$, where $s_a = \theta r^{\alpha}$ and $\mathcal{L}_{I_m}(.)$ is the Laplace transform of $I_m$, which is the interference experienced by the UE from the MTDs outside its S-cell . For analytical tractability, we assume that the set of active MTDs in MX case constitute a HPPP $\Phi_m^{int}$ with density $\lambda_m^{int}$. At a given time, as only one MTD inside a S-cell (if there is any) will be transmitting, the effective density of $\Phi_m^{int}$ will be $\lambda_m^{int} = \lambda_u \times \mathbb{P}\left[N_m \geq 1\right] = \lambda_u(1+\mu)^{-1}$. Hence, we have

$$\begin{aligned}\mathcal{L}_{I_m}(s_a) &= \mathbb{E}\left[\prod_{u_j \in \Phi_m^{int}} \exp\left(-s_a h_j ||u_j||^{-\alpha}\right)\right] \\ &\overset{(b)}{=} \mathbb{E}_Q\left[\exp\left(-2\pi\lambda_m^{int}\int_q^{\infty}\frac{\nu}{1+s_a^{-1}\nu^{\alpha}}d\nu\right)\right],\end{aligned}$$

where $(b)$ follows from the PGFL of PPPs and taking the expectation with respect to $h$ as the channel power gain is independent of $\Phi_m^{int}$. The lower limit of integral $q$ represents the minimum distance separation between the UE and the interfering MTD. Because of the HPPP assumption, this distance is the distance to the nearest UE having at least one MTD in its S-cell. It is Rayleigh distributed according to $f_Q(q) = 2\pi\lambda_m^{int} q \exp\left(-\lambda_m^{int}\pi q^2\right)$. For further simplification, we exploit the convexity of the exponential function and apply Jensen's inequality to shift the expectation operator inside the exponential function to obtain (6).

## References


[1] A. Biral, M. Centenaro, A. Zanella, L. Vangelista, and M. Zorzi, "The challenges of M2M massive access in wireless cellular networks," *Digital Communications and Networks*, vol. 1, no. 1, pp. 1–19, 2015.

[2] H. S. Dhillon, H. C. Huang, H. Viswanathan, and R. A. Valenzuela, "Power-efficient system design for cellular-based machine-to-machine communications," *IEEE Transactions on Wireless Communications*, vol. 12, no. 11, pp. 5740–5753, 2013.

[3] M. Hasan, E. Hossain, and D. Niyato, "Random access for machine-to-machine communication in lte-advanced networks: issues and approaches," *IEEE Communications Magazine*, vol. 51, no. 6, pp. 86–93, 2013.

[4] F. Ghavimi and H.-H. Chen, "M2M communications in 3GPP LTE/LTE-a networks: architectures, service requirements, challenges, and applications," *IEEE Communications Surveys & Tutorials*, vol. 17, no. 2, pp. 525–549, 2015.

[5] Z. Dawy, W. Saad, A. Ghosh, J. G. Andrews, and E. Yaacoub, "Towards massive machine type cellular communications," *arXiv preprint arXiv:1512.03452*, 2015.

[6] X. Lin, J. Andrews, A. Ghosh, and R. Ratasuk, "An Overview of 3GPP Device-to-Device Proximity Services," *IEEE Communications Magazine*, vol. 52, no. 4, pp. 40–48, 2014.

[7] G. Rigazzi, N. K. Pratas, P. Popovski, and R. Fantacci, "Aggregation and trunking of M2M traffic via D2D connections," in *2015 IEEE International Conference on Communications (ICC)*. IEEE, 2015, pp. 2973–2978.

[8] J. G. Andrews, F. Baccelli, and R. K. Ganti, "A tractable approach to coverage and rate in cellular networks," *IEEE Transactions on Communications*, vol. 59, no. 11, pp. 3122–3134, 2011.

[9] R. K. Ganti and M. Haenggi, "Interference and outage in clustered wireless ad hoc networks," *IEEE Transactions on Information Theory*, vol. 55, no. 9, pp. 4067–4086, 2009.

[10] M. Afshang, H. S. Dhillon, and P. H. J. Chong, "Modeling and Performance Analysis of Clustered Device-to-Device Networks," *arXiv preprint arXiv:1508.02668*, 2015.

[11] J. Stienen, *Die Vergroeberung von Karbiden in reinen Eisen-Kohlenstoff-Staehlen*. na, 1982.

[12] R. H. Aquino, S. A. R. Zaidi, D. McLernon, and M. Ghogho, "Modelling and performance evaluation of non-uniform two-tier cellular networks through Stienen model," in *International Conference on Communications (ICC)*. IEEE, 2016.

[13] H. ElSawy, E. Hossain, and M.-S. Alouini, "Analytical modeling of mode selection and power control for underlay D2D communication in cellular networks," *IEEE Transactions on Communications*, vol. 62, no. 11, pp. 4147–4161, 2014.

[14] S. Singh, H. S. Dhillon, and J. G. Andrews, "Offloading in heterogeneous networks: Modeling, analysis, and design insights," *IEEE Transactions on Wireless Communications*, vol. 12, no. 5, pp. 2484–2497, 2013.

[15] S. M. Yu and S.-L. Kim, "Downlink capacity and base station density in cellular networks," in *11th International Symposium on Modeling & Optimization in Mobile, Ad Hoc & Wireless Networks (WiOpt)*. IEEE, 2013, pp. 119–124.